PHYSICAL REVIEW B
CONDENSED MATTER

THIRD SERIES, VOLUME 35, NUMBER 8 15 MARCH 1987-I

New wave-vector selection rule for photoemission from a semi-infinite crystalline solid

B. Craig Meyers and T. E. Feuchtwang
Department of Physics, The Pennsylvania State University, University Park, Pennsylvania 16802
(Received 23 April 1986; revised manuscript received 15 August 1986)

A wave-vector selection rule for photoemission from a semi-infinite periodic solid is derived. The result serves as a model-independent definition of the bulk photoeffect. It is shown that the bulk photocurrent density consists of two contributions. The first contribution may be identified with wave-vector conserving (direct) electronic transitions. The second contribution is due to electronic transitions which do not conserve the "normal" component of wave vector. In general, the two types of transitions produce comparable contributions to the photocurrent density. To illustrate the general results, they are applied to a modified Kronig-Penney model. These calculations illustrate the bulk dependence of the photocurrent density and the relationship of the angle and energy-resolved current density to the band structure. It is noted that for certain experimental configurations, e.g., electron detector angles, it may not be possible to discriminate between bulk and surface effects.

I. INTRODUCTION

The operational separation of the observed photoemission into bulk and surface contributions is a longstanding problem.[1-6] A closely related problem is the formulation of the appropriate wave-vector selection rules applicable to either the bulk or the surface photoeffects.

The purpose of this paper is to derive and discuss the wave-vector selection rules applicable to a semi-infinite as opposed to an infinite periodic solid. In particular, it will be shown that the bulk photocurrent may be separated into two terms. The first, which is due to ("direct") electronic photoexcitations which conserve the three-dimensional wave vector $\mathbf{k}$, is normally identified with the entire bulk component of the photocurrent. However, we shall demonstrate that the second term, which generally is of comparable magnitude, is due to electronic excitations which only conserve the component of the wave vector parallel to the surface, and do not conserve the "normal" component of the wave vector. It should be noted that these selection rules apply generally to any semi-infinite, as opposed to infinite, system. The selection rules are in no way restricted to photoemission which we only chose as a convenient particular example to illustrate their validity. The outline of the paper is as follows.

In Sec. II we derive the wave-vector selection rule. The derivation is based on the scattering-theoretic formulation of photoemission and includes a phenomenological electron extraction length.

In Sec. III, we illustrate the selection rule using a modified Kronig-Penney model. These calculations illustrate the relationship between the experimental configuration and the band structure to be studied, which, in this case, is that of the modified Kronig-Penney model.

In Sec. IV, we present a general discussion which relates our results to experimental data. This discussion is followed by a summary of our conclusions.

II. THE WAVE-VECTOR SELECTION RULES

A. Introduction

In this section we derive the wave-vector selection rules for a semi-infinite periodic solid. We assume the solid to occupy the negative half-space $z<0$, and to be invariant under a group of two-dimensional (lattice) translations of the surface plane $z=0$. We shall apply the scattering-theoretic formulation of photoemission, introduced by Adawi[7] and employed by several others.[1,8,9] This formulation is reviewed below.

B. Scattering theoretical formulation of photoemission

Consider a single electron bound in a semi-infinite periodic solid, described by the "unperturbed" Hamiltonian H_0,

$$(H_0-E)\Phi(\mathbf{r};\mathbf{k},E)=0\ . \tag{1}$$

The eigenfunctions Φ are labeled by the (reduced) wave vector $\mathbf{k}$, and the energy (band index). However, in view of the absence of translational symmetry in the z direction, perpendicular to the surface, Φ is not an eigenfunction of the corresponding component of the (crystal) momentum. Nevertheless, we can label our scattering basis set by the z component of the (reduced) wave vector of the single outgoing beam characterizing these so-called incoming basis functions. We chose to work with the incoming rather than the outgoing scattering states because, as we shall see below, the former are particularly suited to the discussion of photoemission. Using the minimum coupling formulation, the effect of the radiation field on the electronic states $|\mathbf{k},E\rangle$ is described by the perturbation,

$$H'=\frac{ie\hbar}{mc}\mathbf{A}(\mathbf{r};t)\cdot\nabla \ , \tag{2}$$

where $\mathbf{A}$ is the vector potential, and we neglect both the solenoidal and diamagnetic contributions to the photocurrent.[8,9(b)] To lowest order in H' we obtain the following (first Born approximation of the) wave function of the electron emitted with a wave vector $\mathbf{k}_f$ and energy $E_f=E+\hbar\omega$,

$$\Psi(\mathbf{r};\mathbf{k}_f,E_i+\hbar\omega)=\int_\Omega G_0(\mathbf{r},\mathbf{r}';E_i+\hbar\omega)H' \times\Phi(\mathbf{r}';\mathbf{k}_i,E_i)d^3r' \ . \tag{3}$$

Here $\hbar\omega$ is the photon energy and $G_0(\mathbf{r},\mathbf{r}';E)$ is the exact Green function for the unperturbed Hamiltonian H_0, which can be represented by means of the "bilinear formula,"

$$G_0(\mathbf{r},\mathbf{r}';E)=\sum_n \frac{\Phi_n(\mathbf{r})\Phi_n^*(\mathbf{r}')}{E-E_n} \ . \tag{4}$$

For the following, it is helpful to state in some more detail the form of the eigenfunctions $\{\Phi_n\}$, of the field-free Hamiltonian H_0, used in Eq. (4). Each one of these functions consists of a single "outgoing" component traveling away from the surface either in the solid or in the vacuum. We refer to these two types as "outgoing Bloch" and "time-reversed low-energy electron diffraction (LEED)" states, respectively. Both types of wave functions include, in addition, linear combinations of "incoming" waves, traveling to the surface both in the solid and in vacuum. These incoming waves assure the continuity of the complete wave function and of its normal derivative. For the "outgoing Bloch" states, the index n represents the continuous wave vector $\mathbf{k}$, ranging over the positive half of the first Brillouin zone ($k_z\leq 0$), and the discrete energy-band index. For the "time-reversed LEED" states, the index n represents the continuous two-dimensional wave vector, $\mathbf{k}_\rho$, parallel to the surface and the continuous energy. Both types of wave functions conserve the reduced two-dimensional wave vector, $\mathbf{k}_\rho$, parallel to the surface, and are eigenfunctions of the energy. Thus for $z<0$, the eigenfunctions of H_0 include linear combinations of Bloch waves of the form,

$$\phi(m)=\exp(i\mathbf{k}^{(n)}\cdot\mathbf{r})u(\mathbf{r};\mathbf{k}_\rho,E,k_z^{(n)}(\mathbf{k}_\rho,E)) \ . \tag{5}$$

Here, $\mathbf{k}^{(n)}=(\mathbf{k}_\rho,k_z^{(n)})$ and (n) labels the positive roots of

$$k_z=k_z(\mathbf{k}_\rho,E) \ , \tag{6}$$

while u is a periodic function of $\mathbf{r}$. In the vacuum, $z>0$, the eigenfunctions include in addition to the single outgoing plane wave, also combinations of incoming plane waves similar to the incoming Bloch waves specified by Eqs. (5) and (6).

The preceding indicates that the wave function Ψ on the left-hand side of Eq. (3), tends to a simple form in the asymptotic region, $z\gg 0$. Specifically, the wave function of a photoemitted electron observed infinitely far from the solid-vacuum interface is

$$\Psi(\mathbf{r};\mathbf{k}_f,E_f)\sim e^{i\mathbf{k}_f\cdot\mathbf{r}}M_{if} \ . \tag{7}$$

Here the matrix element for photoemission is given by

$$M_{if}=\int\Phi_f^*(\mathbf{r}',E_f=E_i+\hbar\omega)H'(\mathbf{r}')\Phi_i(\mathbf{r}',E_i)d^3r' \ . \tag{8}$$

That is, the final electronic state detected in photoemission tends asymptotically to a plane wave whose amplitude is given by the matrix element M_{if}.

C. Derivation of the wave-vector selection rule

The wave-vector selection rules follow from Eq. (8). The integration indicated in Eq. (8) extends over all space. However, it is obvious that over the exterior half-space, $z>0$, the integrand decreases exponentially with the distance from the surface, z. Thus, in the discussion of bulk photoemission, we may restrict the integration to the semi-infinite solid proper, i.e., $z<0$. We shall denote the corresponding matrix element M_B. From our discussion of the eigenfunctions $\Phi(\mathbf{r},E)$, we conclude that M_B consists of a sum of terms,

$$M_B^{(n,m)}\propto\int_{z\leq 0}\exp[i(\mathbf{k}_i^{(m)}-\mathbf{k}_f^{(n)})\cdot\mathbf{r}]u_f\mathbf{A}\cdot(\nabla+i\mathbf{k}_i)u_i d^3r \ . \tag{9a}$$

This integral can be expressed as an integral over a unit cell and a lattice sum over the semi-infinite solid. Thus, a plane-wave component of the vector potential,

$$\mathbf{A}(\mathbf{r})=\mathbf{a}_0e^{i\mathbf{Q}\cdot\mathbf{r}} \ , \tag{9b}$$

contributes to M_B a term,

$$M_{B,Q}=i\hbar\mathbf{a}_0\cdot{\sum_{\mathbf{R}_n}}'\exp[i(\mathbf{k}_i-\mathbf{k}_f+\mathbf{Q})\cdot\mathbf{R}_n]\mathbf{F} \ . \tag{10}$$

The primed sum is defined by Eq. (15) below. Here we simplified the notation by dropping the indices (m) and (n) labeling the z- components of the wave vectors $\mathbf{k}_i$ and $\mathbf{k}_f$. The factor $\mathbf{F}$ is an integral over the unit cell corresponding to $\mathbf{R}_n=\mathbf{0}$,

$$\mathbf{F}=\int_{\substack{\text{unit}\\ \text{cell}}}\exp[i(\mathbf{k}_i-\mathbf{k}_f+\mathbf{Q})\cdot\mathbf{r}]u_f(\mathbf{r})(i\mathbf{k}_i+\nabla)u_i(\mathbf{r})d^3r \ , \tag{11}$$

and $\mathbf{R}_n$ is a (lattice) vector in the lattice spanned by the basis $\{\mathbf{a}_1,\mathbf{a}_2,\mathbf{a}_3\}$, that is

$$\mathbf{R}_n=\sum_{i=1}^{3}\mathbf{a}_i n_i, \quad n_i=\text{integers} \ . \tag{12a}$$

The basis vector $\mathbf{a}_3$ is chosen to be normal to the surface plane and hence,

$$\mathbf{R}_n=\boldsymbol{\rho}_n+z_n\mathbf{a}_3 \ . \tag{12b}$$

Similarly, we represent the vectors

$$\mathbf{r}=\boldsymbol{\rho}+\mathbf{z}=x_1\mathbf{a}_1+x_2\mathbf{a}_2+z\mathbf{a}_3 \ . \tag{12c}$$

Wave vectors are represented in terms of the basis $\{\mathbf{b}_1, \mathbf{b}_2, \mathbf{b}_3\}$, reciprocal to the basis $\{\mathbf{a}_i\}$, i.e., $\mathbf{a}_i\cdot\mathbf{b}_j=2\pi\delta_{ij}$, and

$$\mathbf{k}=\mathbf{k}_\rho+\mathbf{k}_z=k_1\mathbf{b}_1+k_2\mathbf{b}_2+k_z\mathbf{b}_z \ . \tag{13}$$

Hence,

$$\mathbf{k}\cdot\mathbf{r}=\mathbf{k}_\rho\cdot\boldsymbol{\rho}+2\pi k_z z \ . \tag{14}$$

Thus, the primed lattice sum in Eq. (10) represents the formal three-dimensional sum

$$\sum_{n_1=-\infty}^{\infty}\sum_{n_2=-\infty}^{\infty}\sum_{n_3=-1}^{-\infty}=\sum_{R_n}' \ . \tag{15}$$

In the following we shall be concerned with the interpretation of the "semi-infinite" sum over n_3, for this sum leads to the new selection rules which characterize the bulk emission from a semi-infinite crystal as opposed to the photoexcited current in an infinite solid. Physically, it is convenient to view the semi-infinite solid as the limit of a slab of *effective width* L, and a surface at $z=0$: As L tends to infinity, an increasingly thick slab is being probed by the physical effect being investigated. Tentatively we may identify bulk effects, e.g., photoemission, as explicitly width dependent. Furthermore, they must neither disappear as $L\to\infty$, nor saturate after a small number of unit cells, $n_3=L/a_3$.

In photoemission the effective width of the emitting solid is determined by two phenomenological parameters: the photon absorption coefficient α, and the electronic extraction length L_e. The former is half the probability for photon absorption in the layer extending from z to $z+dz$. The latter is the mean free path for elastic emission of photoexcited electrons. These parameters are, in principle, dependent on the directions of propagation of the photon and electron, respectively. They are treated in the extreme anisotropic limit, in which the photon absorption and electron emission only depend on the component of their respective motions normal to the surface. It is easily seen that the above effects modify Eqs. (10) and (11) as follows:

$$M_{B,Q}(L_e,\alpha)=i\hbar\mathbf{a}_0\cdot\mathbf{F}(L_e,\alpha)\sum_{\rho_n}\sum_{z_n=-1}^{-\infty}\exp[i(\mathbf{k}_{\rho,i}-\mathbf{k}_{\rho,f}+\mathbf{Q}_\rho)\cdot\boldsymbol{\rho}_n+2\pi i(k_{z,i}-k_{z,f}+q_z)z_n+z_n a_3(L_e^{-1}+\alpha)] \ , \tag{16}$$

where

$$\mathbf{F}(L_e,\alpha)=\int_{\text{unit cell}}\exp[i(\mathbf{k}_i-\mathbf{k}_f+\mathbf{Q})\cdot\mathbf{r}+za_3(L_e^{-1}+\alpha)]\times u_f(\mathbf{r})(i\mathbf{k}_i+\nabla)u_i(\mathbf{r})d^3r \ . \tag{17}$$

Here, as stated in Eq. (13), the subscripts ρ and z of the wave vectors denote their components parallel and normal to the surface.

Evidently we may combine L_e and α into an effective extraction length or width L,

$$L^{-1}=L_e^{-1}+\alpha \ . \tag{18}$$

The more general case of a vectorial $\mathbf{L}$ with a nonvanishing component parallel to the surface is treated in Appendix A.

We are now ready to analyze the asymptotic width dependence of the matrix element, which we reiterate, corresponds to the limit of vanishing optical attenuation and arbitrarily large extraction lengths.

Performing the sums indicated by Eq. (16), we obtain

$$M_{B,Q}(L)=-(2\pi)^2 i\hbar\delta(\mathbf{k}_{\rho,i}-\mathbf{k}_{\rho,f}+\mathbf{Q}_\rho)\mathbf{a}_0\cdot\mathbf{F}(L)\times\left[\exp\left[2\pi i(k_{z,i}-k_{z,f}+q_z)a+\frac{a}{L}\right]-1\right]^{-1} . \tag{19}$$

It remains to discuss the asymptotic L dependence, as L tends to infinity, of the last factor on the right-hand side of Eq. (19), which we denote B. In Eq. (19) and the following discussion, the wave vectors k_i and k_f are always reduced (to the first Brillouin zone). Furthermore, we simplify the notation, writing a for $a_3=|\mathbf{a}_3|$, $a/L=\epsilon$ and

$$2\pi i(k_{z,i}-k_{z,f}+q_z)a+\frac{a}{L}=ix+\epsilon \ . \tag{20}$$

Thus we can write the quantity B, introduced above, in the form

$$B(x,L)=-(e^{ix+\epsilon}-1)^{-1} \ . \tag{21}$$

Hence, in the limit, as L tends to infinity,

$$B(x)=\lim_{L\to\infty}B(x,L)=\lim_{\epsilon\to0^+}\frac{ib(x,\epsilon)}{x-i\epsilon} \ , \tag{22}$$

where the function $b(x,\epsilon)$ tends to the limit,

$$\lim_{\epsilon\to0^+}b(x,\epsilon)=1+\frac{ix}{2!}+\cdots \ , \tag{23}$$

which is bounded at $x=0$.

We now apply to Eq. (22) the well-known relation,

$$\lim_{\epsilon\to0^+}\int_0^\infty e^{-i(x-i\epsilon)}dx=-i\lim_{\epsilon\to0^+}(x-i\epsilon)^{-1}=-i\left[\mathrm{P}\left[\frac{1}{x}\right]+\pi i\delta(x)\right] \ , \tag{24}$$

where P denotes the Cauchy principal part. Thus we obtain

$$-\lim_{\epsilon\to 0^+}[\exp(ix+\epsilon)-1]^{-1}=B(x)$$

$$=iP(\mathrm{b}/x)-\pi\delta(x)\ . \quad (25)$$

This result can also be stated as

$$\lim_{\epsilon\to 0^+}[\exp(ix+\epsilon)-1]=P[\exp(ix)-1]^{-1}+\pi\delta(x)\ .$$

We can now discuss the bulk contribution to the matrix element for photoemission which is given by the "bulk limit" of $m_{B,Q}(L)$. Thus, using Eqs. (19)—(25), we obtain

$$\lim_{L\to\infty} M_{B,Q}(L)=(2\pi)^2\hbar\mathbf{a}_0\left[-i\pi\mathbf{F}\delta(\mathbf{k}_i-\mathbf{k}_f+\mathbf{Q})-\mathrm{P}\left[\mathbf{F}\frac{b[2\pi(k_{z,i}-k_{z,f}+q_z)]}{2\pi(k_{z,i}-k_{z,f}+q_z)}\right]\delta(\mathbf{k}_{\rho,i}-\mathbf{k}_{\rho,f}+\mathbf{Q}_\rho)\right]\ . \quad (26)$$

D. Discussion of the bulk limit of the matrix element and photocurrent

Equation (26) presents the contribution to the matrix element for photoemission which persists when the electronic extraction length tends to infinity and the optical absorption tends to zero. This corresponds to the limit of significant photoexcitation arbitrarily far from the surface, and of a reasonable probability for these excited photoelectrons to be emitted across the surface into the vacuum. In the next section we shall demonstrate by means of a model that the qualitative features of the "bulk limit" of the matrix element already emerge for a relatively small effective extraction length L. That is, we shall show that the selection rules indicated by Eq. (26) represent a practical and useful "fingerprint" for bulk photoemission.

The characteristic feature of the "bulk limit" in Eq. (26) is that it consists of two terms. The first term involves a three-dimensional delta function in $\mathbf{k}$, and represents the contribution of the so-called direct transitions.

The second term involves a principal part, which is always associated with the one-dimensional and one-sided delta function defined in Eq. (24).[10] The second factor of this term is a two-dimensional delta function in the parallel wave vectors $\mathbf{k}_\rho$. It imposes the conservation of the components of the wave vectors parallel to the surface. However, the photoinduced electronic transitions contributing to this term do not conserve the component of the wave vector normal to the surface. We refer to these transitions as "directlike."[11]

It should be noted that quite generally the integrated contributions of associated principal part and delta function distributions, such as presented in Eqs. (24) and (26), are of comparable magnitude.[10] Thus, we conclude that the bulk contribution to the photocurrent is due to "direct" and "directlike" electronic transitions. And, in general, these two contributions are of comparable magnitude. Therefore, this suggests that in photoemission spectroscopy, the "direct" peaks are superposed on a background due to a "directlike" contribution which may be misinterpreted as a surface contribution. It follows from Eq. (7) that the photocurrent density is proportional to $|M_{\mathrm{if}}|^2$. It is shown in Appendix B that

$$\lim_{L\to\infty}|M(L)|^2=|\lim_{L\to\infty}M(L)|^2\ .$$

Hence the preceding result, concerning the separate contributions of direct and directlike transitions to the matrix element, applies equally to the photocurrent. Here we note that these two contributions are distinct and no "cross terms" appear in the current.

III. ILLUSTRATION OF THE WAVE-VECTOR SELECTION RULES

A. The model

In this section we apply numerical methods to analyze the matrix element for a simple model. The purpose of these calculations is to demonstrate that the selection rules for bulk photoemission are indeed satisfied, and that they are approximately satisfied even for small values of the effective electronic extraction length L. The calculation utilizes the modified Kronig-Penney (KP) model for which the potential $V(\mathbf{r})$ is

$$V(\mathbf{r})=\begin{cases}0, & z>0\ ,\\ \dfrac{\hbar^2}{2m}\dfrac{2P}{a}\displaystyle\sum_{n=0}^{-\infty}\delta(z+na+b)+V_0, & z<0\ .\end{cases} \quad (27)$$

Here, P is a dimensionless potential. The lattice parameter previously denoted $|\mathbf{a}_3|$ is denoted "a." The surface is located at b. The three-dimensional potential $V(\mathbf{r})$ is only a function of z, and hence, the Schrödinger equation for this quasi-three-dimensional model is trivially separable.

In the following, we also replace the single plane-wave component of the vector potential, defined by Eq. (9), with a more complete asymptotic representation of the field associated with a single plane-wave incident from the vacuum. That is, following Melnyk and Harrison,[12] we write

$$\mathbf{A}(r)=\begin{cases}\hat{\boldsymbol{\epsilon}}_T a_0 T\exp[-i(\mathbf{Q}_\rho\cdot\boldsymbol{\rho}+q_T z)]+\hat{\boldsymbol{\epsilon}}_L a_0\tilde{L}\exp[-i(\mathbf{Q}_\rho\cdot\boldsymbol{\rho}+q_L z)], & z<0\ ,\\ \hat{\boldsymbol{\epsilon}}_I a_0\exp[-i(\mathbf{Q}_\rho\cdot\boldsymbol{\rho}+qz)]+\hat{\boldsymbol{\epsilon}}_R a_0 R\exp[-i(\mathbf{Q}_\rho\cdot\boldsymbol{\rho}-qz)], & z>0\ .\end{cases} \quad (28)$$

Here, $\hat{\epsilon}_I$, $\hat{\epsilon}_R$, $\hat{\epsilon}_T$, and $\hat{\epsilon}_L$ are polarization vectors for the incident, reflected, transmitted transverse and transmitted longitudinal electromagnetic fields, respectively. The corresponding field amplitudes are a_0, a_0R, a_0T, and $a_0\tilde{L}$. The wave vectors for these fields are $\mathbf{Q}_I=(\mathbf{Q}_\rho,q)$, $\mathbf{Q}_R=(\mathbf{Q}_\rho,-q)$, $\mathbf{Q}_T=(\mathbf{Q}_\rho,q_T)$, and $\mathbf{Q}_L=(\mathbf{Q}_\rho,q_L)$. The wave vector for the transmitted transverse field, $\mathbf{Q}_T$, is obtained from the dispersion relation,

$$\epsilon_T(\mathbf{Q}_T,\omega)=\left[\frac{c}{\omega}\right]^2\mathbf{Q}_T\cdot\mathbf{Q}_T \ . \tag{29}$$

The wave vector of the transmitted longitudinal wave is obtained from

$$\epsilon_L(\mathbf{Q}_L,\omega)=0 \ . \tag{30}$$

The functions ϵ_T and ϵ_L are the dielectric functions for the transverse and longitudinal fields derived, e.g., by Melnyk and Harrison.[12]

Thus, the matrix element for photoemission is given by

$$M_{if}(\mathbf{k}_i,E_i;L)=\frac{e}{mc}\int_\Omega \Phi_f^*(\mathbf{r},\mathbf{k}_f)e^{za_3L^{-1}}\mathbf{A}\cdot\mathbf{p}\Phi_i(\mathbf{r},\mathbf{k}_i)d^3r \ , \tag{31}$$

where we have included the phenomenological effective electronic extraction length, which allows us to study the evolution of the bulk effect with increasing L. It should be noted that in Eq. (31) the matrix element is an integral over all space.

B. Numerical results

In the calculations discussed below we used the following values for the parameters introduced in Sec. III A above: $a=5.65$ a.u., $b=0.0$ a.u., $P=0.30$, $V_0=5.56$ eV. These values are characteristic for Na, for which the Fermi energy is $E_F=3.24$ eV, the work function is $\phi=2.32$ eV, and the plasma energy is $\hbar\omega_p=5.75$ eV. This modified KP model potential has been used previously by Schaich and Ashcroft[13] in an illustration of their quadratic response formulation of photoemission. The same model was also used by Meyers and Feuchtwang in a discussion of band-gap photoemission.[14]

1. The direct transition

In Fig. 1 we present angle-resolved energy distribution curves (AREDC's) for several values of the effective electronic extraction length L. These plots present the photocurrent per unit solid angle as a function of the angle between the detector axis and the surface normal. In the following, we refer to this angle θ, as the detector angle. The photon energy is $\hbar\omega=4.0$ eV and the constant final energy is $E_f=1.4$ eV.[15] That is, as θ varies from 90° to 0° the initial "normal" energy,

$$\tilde{E}_i=E_i-\frac{\hbar^2k_\rho^2}{2m}=E_f-\hbar\omega-E_f\sin^2\theta \ , \tag{32}$$

is scanned over the interval $-4\le\tilde{E}_i\le-2.6$ eV. The characteristic features of Fig. 1 are the following:

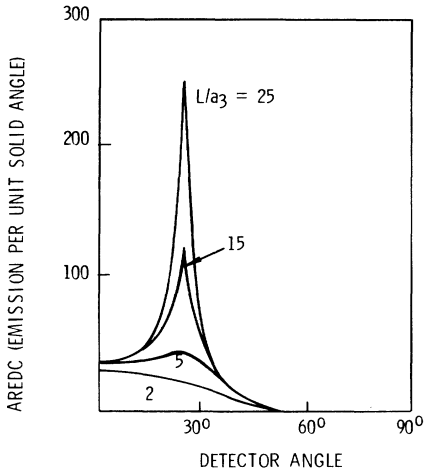

FIG. 1. Angle-resolved energy distribution curves (AREDC's) at constant final state and photon energy for a modified Kronig-Penney model, and several values of the effective electronic extraction length L/a_3. The curves are labeled by the appropriate L/a_3.

(1) The featureless AREDC at low L, develops an increasingly pronounced peak as L increases. This peak completely dominates the AREDC for large values of L.[16]

(2) The detector angle at which the peak occurs is independent of L.

These features of the AREDC can be interpreted in terms of the electronic (bulk) energy band structure of the modified KP model, presented in Fig. 2. In this figure we also indicate several transitions which are labeled by the detector angle θ, at which they are probed. The peak in Fig. 1 occurs at $\theta=26°$ and corresponds to the *only* direct transition observable for the particular set of parameters considered. All the other transitions (two of which are indicated in Fig. 2) which contribute to the AREDC are "directlike", and not "direct." The existence of at most a single direct transition for any given constant photon and final electron energies is characteristic of our separable quasi-three-dimensional model.

The calculations were done for a photon angle of incidence of 30°. The calculation is inherently sensitive to the photon angle of incidence because of the Q dependence of the field amplitudes T and $\tilde{L}$, in Eq. (28). In contrast, the Q dependence in the selection rules can be neglected. The most dramatic illustration of the Q sensitivity of photoemission occurs when the angle of incidence equals (or exceeds) the critical angle, i.e., "total reflection" sets in, and the z components of the wave vectors in the metal acquire an imaginary part.[8] We expect the results above to apply, qualitatively, also for angles of incidence larger than the critical angle. However, the sharpness of the direct transition peak should diminish with increasing angle of incidence, as the delta function, $\delta(k_{z,i}-k_{z,f}+q_z)$ tends to a Lorentzian

$$[\mathrm{Im}(k_{z,i}-k_{z,f})+\mathrm{Re}(q_z)+i\,\mathrm{Im}(q_z)]^{-1} \ .$$

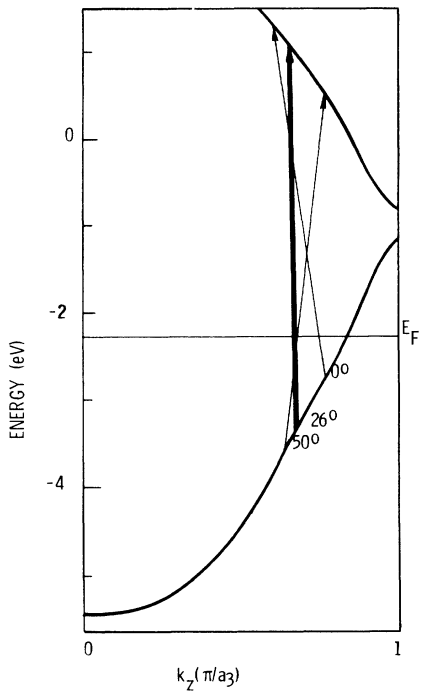

FIG. 2. Electronic energy band structure $\tilde{E}(k_z)$ of the modified Kronig-Penney model. The normal energy, $\tilde{E}$, is referred to the vacuum level. The arrows represent typical electronic transitions, induced by the absorption of a photon of energy $\hbar\omega=4$ eV, and contributing to the AREDC's in Fig. 1. The transitions are labeled by the detector angle at which they emerge from the solid. The heavy arrow denotes the only direct transition at this photon energy while the light arrows represent directlike contributions to the AREDC.

The direct transition peak in the AREDC clearly exhibits a dependence on the extraction length, as expected, on the basis of the discussion in Sec. II above, for bulk photoemission. We now turn to examine the L dependence of the balance of the AREDC.

2. *The "directlike" transitions*

The direct peak rides on a background, which close to the peak, is strongly L dependent. This L dependence is expected for a bulk effect. However, as seen from Fig. 1, for $\theta \gtrsim 40°$, the background is virtually L independent. The explanation of the unexpected behavior of this bulk "directlike" contribution to the AREDC is quite simple. For $\theta \gtrsim 40°$

$$|\Delta\mathbf{k}_z|\, a_3 = 2\pi\, |k_{z,f}-k_{z,i}|\, a \gtrsim 0.08\pi \ . \tag{33}$$

Thus, neglecting the photon wave vector compared to the electronic wave vectors, we conclude from Eqs. (9), (19), and (31) that the matrix element

$$M(\mathbf{k}_i,E_i;L) \propto [\exp(i\,2\pi\Delta k_z a + a_3/L)-1]^{-1} \ . \tag{34}$$

The photocurrent density is proportional to the squared magnitude of the matrix element,

$$J(L) \propto \left[\exp\frac{2a_3}{L} - 2\cos 2\pi\Delta k_z a \exp\frac{a_3}{L} + 1\right]^{-1} \ . \tag{35}$$

Equation (35) indicates, in agreement with Fig. 1, that when

$$|\Delta\mathbf{k}_z|\,\frac{a_3}{\pi} = 2\Delta k_z a \gtrsim 0.1$$

and $L \gtrsim 5a_3$, then the contribution of the directlike transitions to the photoemitted current density loses its sensitivity to the electronic extraction length L. That is, both Eq. (35) and Fig. 1 suggest that the directlike contribution to the AREDC tends to peak and to become strongly L dependent as $|\Delta\mathbf{k}_z|\, a_3 \to 0$, i.e., as the direct transition peak is approached. However, in contrast, far from a direct transition peak the directlike and surface contributions to the AREDC cannot be unambiguously separated. That is, both contributions fail to conserve the normal (z) component of the wave vector and both tend to saturate for small values of the extraction length, $L/a_3 \sim 1-2$. The last observation was confirmed by calculations of AREDC's to which only directlike transitions could contribute. Here it should be reiterated that these contributions were calculated from the *bulk* energy-band structure.

IV. DISCUSSION

The wave-vector selection rule specified by Eq. (26) states that the bulk photoeffect is due to both direct and directlike photoexcited electronic transitions. These two contributions to the photocurrent density are comparable, as illustrated by the calculated AREDC's in Fig. 1.

Thus, we are led to a quasioperational definition of the bulk photoeffect: A relatively sharp peak in the AREDC is a signature of bulk direct transitions. This does not exclude the possibility of a surface transition which accidentally conserves k_z. However, it asserts that a high probability of k_z conservation is characteristic of a bulk one-electron photoexcitation. Consequently, any spectral structure with significant integrated intensity that can be associated with a wave vector conserving transition may be interpreted as a bulk effect. Furthermore, these direct transition peaks can be distinguished from other structures, presumably due to either strictly surface effects or bulk-surface interference effects, by their relative insensitivity to surface modifications, e.g., by adsorbates and defects. The preceding comment clearly refers to effects that are localized at the surface to within a few interatomic distances. However, the very existence of a surface has long-range consequences, such as the occurrence of directlike transitions due to the breaking of the translational symmetry normal to the surface. Logically one has to consider such effects as bulk phenomena characteristic of the semi-infinite, as opposed to the infinite, crystal. In other words, in general, surface effects are only those that are not interpretable in terms of the bulk energy-band structure and hence, do not probe it.[17] There is a high probability that surface photoexcitations do not conserve the normal component of the wave vector. However, the absence of significant structure in the AREDC does not necessarily exclude the contribution of bulk, directlike

transitions to the spectrum. The operational disentanglement of the directlike from the surface contributions has been discussed in Sec. III.

The fact that directlike transitions do not give rise to pronounced structure in the AREDC suggests that they may have to be considered only in the analysis of the line shapes.

V. SUMMARY

Wave-vector selection rules for photoemission from a semi-infinite crystalline solid were derived. The rules were derived in terms of a "bulk limit" in which the effective width L of the semi-infinite sample tends to infinity. Bulk effects were thus identified as nonsaturating for small L and persisting for arbitrarily large L. It was shown that the bulk photoeffect consists of two comparable contributions. The first is due to wave-vector-conserving, direct, electronic transitions. The second contribution is due to directlike electronic transitions that conserve only the component of the wave vector parallel to the surface. An illustration of the selection rule was provided by a numerical analysis of a modified Kronig-Penney model. The bulk photoeffect was shown to lead to a peak in the constant final-state AREDC, and the peak was identified with the direct transition. However, the calculations suggest that, in general, the separation of surface and directlike contributions to the photoemitted current density may be more difficult than previously recognized. It should be emphasized that the selection rules derived in this paper apply generally to any semi-infinite as opposed to infinite system. That is, these selection rules are not restricted to photoemission, which we chose simply as a convenient example to illustrate our results.

ACKNOWLEDGMENTS

This research was supported in part by the Applied Research Laboratory of The Pennsylvania State University, under Grant No. E/F6161.

APPENDIX A: PROOF OF SELECTION RULE FOR VECTORIAL EXTRACTION LENGTH

In the text we assumed that both the photoabsorption and the mean free path for the elastic emission of photoexcited electrons depend only on the normal, or z component of the path. We shall now drop this assumption, i.e., we shall introduce the vectorial inverse effective extraction length,

$$\mathbf{L}^{-1}=\sum_{j=1}^{3} L_j^{-1}\mathbf{b}_j \ , \tag{A1}$$

where $\{\mathbf{b}_1,\mathbf{b}_2,\mathbf{b}_3\}$ is the basis reciprocal to $\{\mathbf{a}_1\mathbf{a}_2,\mathbf{a}_3\}$, the basis introduced by Eq. (12). Instead of the sums over n_1 and n_2 in Eq. (15), we now have to evaluate the two-dimensional sum,

$$\begin{aligned}\lim_{L_1^{-1},L_2^{-1}\to 0}\sum_{n_1=-\infty}^{\infty}\sum_{n_2=-\infty}^{\infty}\exp\left[2\pi i\sum_{j=1}^{2}[(k_{j,i}-k_{j,f}+Q_j)n_j+i\,|\,L_j^{-1}n_j\,|\,]\right]\\ =\prod_{j=1}^{2}\lim_{L_j^{-1}\to 0}(\{1-\exp[2\pi i(k_{j,i}-k_{j,f}-Q_j+iL_j^{-1})]\}^{-1}+\{1-\exp[-2\pi i(k_{j,i}-k_{j,f}-Q_j-iL_j^{-1})]\}^{-1}-1)\\ =\delta(\mathbf{k}_{\rho,i}-\mathbf{k}_{\rho,f}+\mathbf{Q}_\rho+\mathbf{G}_\rho)\ ,\end{aligned} \tag{A2}$$

where $\mathbf{G}_\rho$ is a two-dimensional reciprocal-lattice vector.

That is, conservation, modulo a two-dimensional reciprocal-lattice vector, of the components of the (reduced) wave vectors parallel to the surface is unaffected by the vectorial inverse extraction length. It is the semi-infinite extent of the solid in the normal direction that leads to the partial nonconservation of the normal component of the wave vector even in the limit $L_3\to\infty$.

The extension of the preceding results from the semi-infinite solid to the finite-sized crystal is obvious, and is therefore omitted.

APPENDIX B: EVALUATION OF $\lim_{L\to\infty}|M_{B,Q}(L)|^2$

In this appendix we demonstrate that

$$\lim_{L\to\infty}|M_{B,Q}(L)|^2=|\lim_{L\to\infty}M_{B,Q}(L)|^2\ . \tag{B1}$$

That is, the limit $L\to\infty$ is well defined, even though it is applied to products of distributions rather than ordinary functions. In order to interpret the right-hand side of Eq. (B1), we note that

$$\begin{aligned}\left|\lim_{L\to\infty}M(L)\right|^2&=\left|\lim_{L\to\infty}\frac{b(x,L)}{(x-ia/L)}\right|^2\\ &=\left|\mathrm{P}\left[\frac{b}{x}\right]+\pi i\delta(x)\right|^2\\ &=\left[\mathrm{P}\left[\frac{|\,b\,|}{x}\right]\right]^2+[\pi\delta(x)]^2\ ,\end{aligned} \tag{B2}$$

where $x=2\pi(k_{z,i}-k_{z,f}+q_z)$ and $\mathrm{P}(1/x)\delta(x)\equiv 0$. We now have to interpret the squared distributions in Eq. (B2). First, we note the well-known differential formula,[18]

$$\mathrm{P}\left[\frac{1}{x^2}\right]=-\frac{d}{dx}P\left[\frac{1}{x}\right], \tag{B3}$$

and the definitions of $\mathrm{P}(1/x)$, $\delta(x)$:

$$\mathrm{P}\left[\frac{1}{x}\right]=\lim_{\epsilon\to 0}\frac{x}{x^2+\epsilon^2}, \tag{B4}$$

$$\pi\delta(x)=\lim_{\epsilon\to 0}\frac{\epsilon}{x^2+\epsilon^2}. \tag{B5}$$

Hence,

$$\mathrm{P}\left[\frac{1}{x^2}\right]=\lim_{\epsilon\to 0}\frac{x^2-\epsilon^2}{(x^2+\epsilon^2)^2}=\left[\mathrm{P}\left[\frac{1}{x}\right]\right]^2-[\pi\delta(x)]^2. \tag{B6}$$

Next we apply the standard interpretation of the square of the delta function,[19] to reduce Eq. (B2) to

$$\left|\lim_{L\to\infty}M(L)\right|^2=\mathrm{P}\left[\frac{|b|}{x}\right]^2+2[\pi\delta(x)]^2, \tag{B7}$$

$$=\mathrm{P}\left[\frac{|b|}{x}\right]^2+2\frac{L}{a}\pi\delta(x). \tag{B8}$$

Finally, applying once more Eqs. (B5) and (B6)

$$\lim_{L\to\infty}|M(L)|^2=\lim_{L\to\infty}\frac{|b(x,L)|^2}{x^2+(a/L)^2}$$

$$=\mathrm{P}\left[\frac{|b|}{x}\right]^2+2[\pi\delta(x)]^2. \tag{B9}$$

Combining Eqs. (B8) and (B9), we obtain Eq. (B1).

[1] M. L. Glasser and A. Bagchi, Prog. Surf. Sci. **7**, 113 (1976).

[2] B. Feuerbacher and R. F. Willis, J. Phys. C **9**, 169 (1976).

[3] N. V. Smith, CRC Crit. Rev. Solid. State Sci. **2**, 45 (1971).

[4] D. E. Eastman, in *Techniques of Metals Research*, edited by E. Passaglia (Interscience, New York, 1972), Part I, p. 411.

[5] M. Cardona and L. Ley, *Topics in Physics* (Springer-Verlag, Berlin, 1978), Vol. 26.

[6] T. E. Feuchtwang, P. H. Cutler, and J. Schmit, Surf. Sci. **75**, 401 (1978).

[7] I. Adawi, Phys. Rev. **134**, A788 (1964).

[8] B. C. Meyers and T. E. Feuchtwang, Phys. Rev. B **27**, 2030 (1983).

[9] (a) G. D. Mahan, Phys. Rev. B **2**, 4334 (1970); (b) C. Caroli, D. Leder-Rosenblatt, B. Roulet, and D. Saint-James, *ibid.* **8**, 4552 (1973).

[10] This is a well-known result from the calculus of residues. See, for example, (a) E. T. Copson, *An Introduction to the Theory of Functions of a Complex Variable* (Oxford, London, 1950); or (b) P. M. Morse and H. Feshbach, *Methods of Mathematical Physics* (McGraw-Hill, New York, 1953), p. 368.

[11] Here, and in the following, the electronic transitions are said to conserve the αth component of wave vector if $k_{\alpha,i}=k_{\alpha,f}-Q_\alpha$. This terminology implies correctly that the photon's wave vector is normally negligible compared to the electronic wave vectors. However, strictly speaking, it is not just the electronic transition but the electron-photon system that conserves the α component of the wave vector.

[12] A. R. Melnyk and M. J. Harrison, Phys. Rev. B **2**, 835 (1970); **2**, 851 (1970).

[13] W. L. Schaich and N. W. Ashcroft, Phys. Rev. B **3**, 2452 (1971).

[14] B. C. Meyers and T. E. Feuchtwang, Phys. Rev. B **28**, 2212 (1983).

[15] Note that the photon energy $\hbar\omega$ is below the bulk plasmon energy $\hbar\omega_p$. The particular choice of photon energy was made to illustrate transitions from the initial band of occupied states to the lowest band of unoccupied excited states. The contribution of the nonpropagating longitudinal field excited by the incident field on the metal side of the interface [see Eq. (28)] has been explicitly included, along with the propagating, transmitted transverse field, in the calculation of the matrix element. Thus, our results explicitly apply to photon energies $\hbar\omega\leq\hbar\omega_p$.

[16] In comparing our Fig. 1 with Fig. 3 of Ref. 13, slight differences are noted. Thus, for an extraction length $L=5$, Schaich and Ashcroft (SA) have no structure in the AREDC for a detector angle $\theta\sim 26°$ although they report a small peak in the AREDC for a detector angle $\theta\sim 50°$. The reason for the difference is that we have included, besides the incident field, also the Q-dependent field amplitudes R, T, and L, which were not considered by SA. Thus, SA implicitly took $R=0$, $T=1$ for all photon wave vectors.

[17] The notable exception to this characterization of surface effects is the so-called gap emission, i.e., emission of electrons photoexcited into states of energy in forbidden bulk energy gaps. This surface effect which, in fact, probes the bulk energy-band structure is discussed in Ref. 14.

[18] R. P. Kanwal, *Generalized Functions: Theory and Technique* (Academic, New York, 1983), p. 88, Eq. 13.

[19] A. Messiah, *Quantum Mechanics* (Wiley, New York, 1962), Vol. II, p. 1047.